



# MUR: Momentum Uncertainty guided Reasoning for Large Language Models

Hang Yan<sup>◇\*</sup> Fangzhi Xu<sup>◇\*†</sup> Rongman Xu<sup>◇</sup> Yifei Li<sup>◇</sup> Jian Zhang<sup>◇♡</sup> Haoran Luo<sup>♡</sup>  
 Xiaobao Wu<sup>♡</sup> Luu Anh Tuan<sup>♡</sup> Haiteng Zhao<sup>♣†</sup> Qika Lin<sup>♣</sup> Jun Liu<sup>◇†</sup>  
<sup>◇</sup>Xi'an Jiaotong University <sup>♡</sup>Nanyang Technological University  
<sup>♣</sup>Peking University <sup>♣</sup>National University of Singapore  
 hyan@stu.xjtu.edu.cn, fangzhixu98@gmail.com, zhaohaiteng@pku.edu.cn  
 liukeen@xjtu.edu.cn

\* means equal contribution

† denotes corresponding authors

⌚ <https://github.com/yayayacc/MUR>

## Abstract

Large Language Models (LLMs) have achieved impressive performance on reasoning-intensive tasks, yet optimizing their reasoning efficiency remains an open challenge. While Test-Time Scaling (TTS) improves reasoning quality, it often leads to overthinking—wasting tokens on redundant computations. This work investigates *how to efficiently and adaptively guide LLM test-time scaling without additional training*. Inspired by the concept of momentum in physics, we propose Momentum Uncertainty-guided Reasoning (*MUR*), which dynamically allocates thinking budgets to critical reasoning steps by tracking and aggregating step-wise uncertainty over time. To support flexible inference-time control, we introduce  $\gamma$ -control, a simple mechanism that tunes the reasoning budget via a single hyperparameter. We provide in-depth theoretical proof to support the superiority of *MUR* in terms of stability and biases. *MUR* is comprehensively evaluated against various TTS methods across four challenging benchmarks (MATH-500, AIME24, AIME25, and GPQA-diamond) using different sizes of recent Qwen3 models (1.7B, 4B, and 8B). Results demonstrate that *MUR* reduces computation by over 50% on average while improving accuracy by 0.62–3.37%.

## 1 Introduction

Large Language Models (LLMs) Brown et al. (2020); Dubey et al. (2024) demonstrate remarkable performance in reasoning-intensive scenarios, including logic, mathematics, and game-playing tasks. A critical advancement in optimizing their reasoning quality is *Test-Time Scaling* (TTS). Existing methods either incentivize long thinking patterns through reinforcement learning with verifiable rewards (RLVR) Ye et al. (2025); Jaech et al. (2024); Guo et al. (2025), or employ stepwise optimization via parallel sampling Yao et al. (2023); Lightman et al. (2023); Wang et al. (2024b); Ma et al. (2024); Xu et al. (2025a) and sequential critique Lan et al. (2024); Li et al. (2025).

While effective, the issue of *overthinking* Chen et al. (2024b); Sui et al. (2025) is widely observed that degrades the inference efficiency. As shown in Figure 1, the performance can even be slightly improved, despite >50% reduction in thinking tokens. This demonstrates that there is significant room for improvement in making long thinking concise.

Intuitively, LLMs should spend more token budgets on complex steps to deliberately enhance output quality, while generating simple steps directly to avoid overthinking.

Thus, it still remains challenging to identify key steps and dynamically allocate computes. Recent works [Xia et al. \(2025a\)](#); [Jiang et al. \(2025\)](#); [Yang et al. \(2025c\)](#); [Yu et al. \(2025\)](#); [Yang et al. \(2025b\)](#) explore training methods to adaptively allocate token usage on different steps, which introduce additional training costs and lack generalization. Off-the-shelf training-free methods [Kim et al. \(2025\)](#); [Xu et al. \(2025a\)](#); [Wang et al. \(2025\)](#) scale thinking tokens in a fixed manner, failing to adapt to problem complexity or on-going reasoning process. Therefore, the pursuit of efficiently and adaptively guiding LLM test-time scaling without training is both intriguing and understudied.

To answer this question, we are the first to model LLM reasoning with the concept of momentum. In physics, momentum accumulates historical information over time and resists sudden changes. Based on this and the successful application of Gradient Descent with Momentum [Qian \(1999\)](#), we propose Momentum Uncertainty guided Reasoning (*MUR*), a novel approach that dynamically evaluates the overall uncertainty of a reasoning path by aggregating historical step-level uncertainties, mirroring the smooth and consistent evolution observed in physical dynamics. Without requiring any training, *MUR* selectively allocates computation only to critical steps during inference. Based on the approach, we introduce the concept of  $\gamma$ -control, where we can flexibly control the thinking budget and the performance, with only one hyperparameter  $\gamma$ . Further, this work proves that *MUR* is theoretically grounded in terms of discounted credit assignment, stability, and convergence while maintaining compatibility with existing TTS methods. Extensive experiments across four challenging benchmarks and three backbone model sizes demonstrate that *MUR* reduces the thinking budget by over 50% on average while even improving accuracy by 0.62–3.37%.

The key contributions include:

- (1) **Adaptive Scaling Technique.** We propose a novel concept of momentum uncertainty and offer a training-free solution *MUR* to dynamically allocate computes to key reasoning steps guided by momentum uncertainty, which is compatible with various TTS methods.
- (2) **Efficiency and Performance Gains:** *MUR* reduces the thinking costs by 50% even with obvious performance gains, across a wide range of benchmarks and model sizes. The proposed  $\gamma$ -control offers flexible solution to balance performance and efficiency.
- (3) **Theoretical Support:** *MUR* is theoretically grounded in terms of discounted credit assignment, stability, and convergence, which support its practical superiority.

## 2 Related Work

### 2.1 Test-Time Scaling

Test-Time scaling (TTS) methods allocate additional token usage during inference, revealing a scaling law [Brown et al. \(2024\)](#); [Wu et al. \(2024\)](#) that more computes lead to better performance. Training-based methods elicit long thinking patterns through reinforcement learning with verifiable rewards (RLVR) [Ye et al. \(2025\)](#); [Jaech et al. \(2024\)](#); [Guo et al. \(2025\)](#). Training-free methods can be categorized into parallel scaling and sequential scaling. Parallel scaling [Yao et al. \(2023\)](#); [Ma et al. \(2024\)](#); [Xu et al. \(2025a\)](#) samples several answers for the same input, followed by selecting the best one. Sequential scaling [Lan et al. \(2024\)](#); [Li et al. \(2025\)](#) utilizes feedback from self-evaluation or external models to optimize current an-

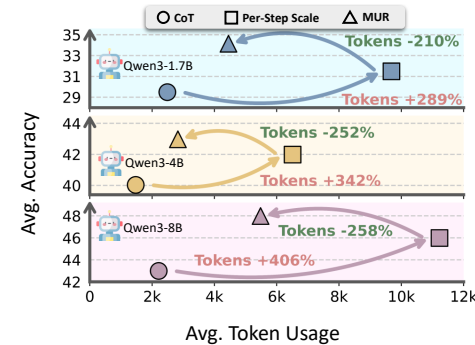


Figure 1: Comparisons between average accuracy and token usage. *Per-Step Scale* refers to test-time scaling methods that optimize every step without compute-saving mechanisms. *MUR* is a computationally efficient approach that selectively scales only key steps.

swer. Although these researches show remarkable achievements, they allocate unnecessary computes for simple steps. Our work *MUR*, as an orthogonal method to these researches, optimizing test-time scaling methods by guiding them to scale only the key steps, reducing unnecessary computes largely.

## 2.2 Overthinking

Although LLMs demonstrate significant performance gains through test-time scaling methods, they are likely to introduce computational overhead and reasoning latency [Chen et al. \(2024b\)](#); [Sui et al. \(2025\)](#). One line of mitigating overthinking is to shorten reasoning length through post-training [Xia et al. \(2025a\)](#); [Jiang et al. \(2025\)](#); [Yang et al. \(2025c\)](#); [Yu et al. \(2025\)](#); [Yang et al. \(2025b\)](#), which introduces training overhead and limits their generalization. Another line is training-free methods [Kim et al. \(2025\)](#); [Xu et al. \(2025a\)](#); [Wang et al. \(2025\)](#), reducing token usage in a fixed manner, which lacks adaptation to the on-going reasoning process. Our work *MUR*, as a training-free method, adaptively saves unnecessary computes during the whole reasoning process.

## 2.3 Uncertainty Estimation

The reasoning path of LLM often contains reliability issues, like hallucinations or biased responses [Xia et al. \(2025b\)](#). One line of uncertainty estimation is scaling more computes, including verbalizing methods [Tian et al. \(2023\)](#); [Tanneru et al. \(2024\)](#), consistency-based methods [Hou et al. \(2024\)](#); [Chen & Mueller \(2024\)](#); [Gao et al. \(2024\)](#), and semantic clustering methods [Kuhn et al. \(2023\)](#); [Farquhar et al. \(2024\)](#); [Nikitin et al. \(2024\)](#). Another line of uncertainty estimation is utilizing the internal information during decoding [Ahdritz et al. \(2024\)](#); [Chen et al. \(2024a\)](#); [Sriramanan et al. \(2024\)](#); [Xu et al. \(2025b\)](#), which estimates the uncertainty of generated path through aggregating token-level probabilities, lacking the adaptation to different reasoning steps. Our method *MUR*, assigns more attention to recent steps, while reducing the impact of early steps.

## 3 Method

In this section, we first formulate the stepwise test-time scaling, adaptive scaling and step-level uncertainty (Sec. 3.1). Then we formally propose momentum uncertainty, followed by theoretical proof of its superiority (Sec. 3.2). Based on the momentum uncertainty, we introduce  $\gamma$ -control mechanism to flexibly scale inference-time scaling (Sec. 3.3). The overview of *MUR* is presented in Figure 2.

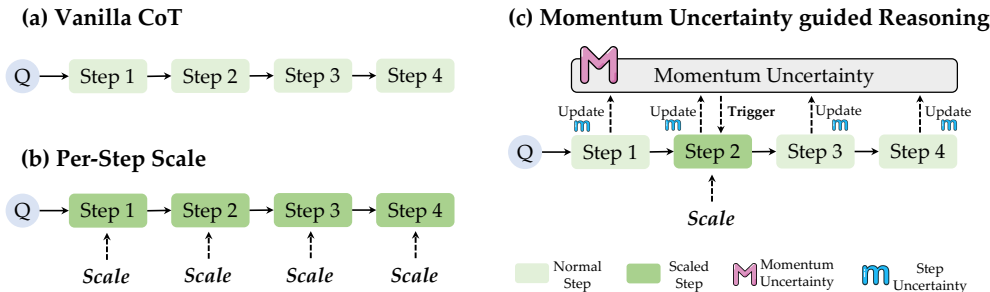


Figure 2: Comparison of reasoning methods. (a) *Vanilla CoT*: Standard stepwise reasoning without test-time scaling. (b) *Per-Step Scale*: scales computes per reasoning step. (c) *MUR*: Adaptive test-time scaling framework (ours).

### 3.1 Preliminary

**Stepwise test-time scaling** LLM reasoning can be formulated as auto-regressively generating step  $a_t$  at each timestamp  $t$ , based on the inputs and previous steps:

$$a_t \sim p_\theta(\cdot|x, \mathbf{a}_{<t}), \quad (1)$$

where  $x$  is the concatenation of input question and instruction.  $\mathbf{a}_{<t}$  represents previous steps.  $\theta$  denotes the parameters of pre-trained LLM, and  $p_\theta$  is the probability distribution.

To optimize the quality of the reasoning path, current methods apply test-time scaling at each step, which can be formulated as follows:

$$\hat{a}_t \sim Q(\cdot|x, \mathbf{a}_{<t}), \quad (2)$$

where  $\hat{a}_t$  is the optimized step.  $Q$  denotes the specific test-time scaling method, such as *Best-of-N* Brown et al. (2024).

**Adaptive Scaling** Conventional test-time scaling methods typically apply optimization at every decoding step, leading to excessive token usage and computational overhead. However, not all steps require such enhancement, and current research on adaptive compute allocation remains limited, often overlooking this inefficiency. We therefore pose the central question: *When should compute be scaled during inference?* To address this, we model this research question with a binary detector  $D$  that selectively activates test-time scaling based on contextual reasoning dynamics:

$$\hat{a}_t = \begin{cases} Q(\cdot|x, \mathbf{a}_{<t}) & , D(t) = \text{True} \\ a_t & , D(t) = \text{False} \end{cases}. \quad (3)$$

Here,  $D$  determines whether to invoke a test-time scaling method at each step based on historical information. Our work focuses **exclusively** on designing the detector  $D$  to assess the reasoning trajectory and adaptively decide whether to allocate additional compute to the current step  $a_t$ .

**Step-level Uncertainty** Uncertainty estimation quantifies an LLM’s confidence in its output, where higher uncertainty implies lower confidence. For step  $a_t$  consisting of  $N$  tokens, we compute the step-level uncertainty based on token-wise probabilities. Specifically, we define the average negative log-likelihood of the tokens as:

$$m_t = \frac{1}{N} \sum_{j=1}^N -\log p_\theta(a_t^{(j)}|x, \mathbf{a}_{<t}, a_t^{(<j)}), \quad (4)$$

where  $m_t$  the uncertainty of step  $t$ .  $a_t^{(j)}$  is  $j$ -th token of step  $a_t$ . And  $a_t^{(<j)}$  denotes the prefix token sequence  $a_t^{(1)}, a_t^{(2)}, \dots, a_t^{(j-1)}$ .

### 3.2 Momentum Uncertainty

LLM can maintain an uncertainty estimation  $M$  for the reasoning process, reflecting the global assessment of both input  $x$  and generated steps  $\mathbf{a}_{<t}$ . Ideally, this uncertainty should evolve smoothly, adapting to new steps, as they are generated while preserving a calibrated estimate of earlier steps. Inspired by the concept of momentum in physics, which retains and updates an object’s motion by accumulating past forces while resisting abrupt changes. We propose momentum uncertainty, a recursive formulation of  $M$  that dynamically tracks overall uncertainty during reasoning as follows:

$$M_t = \alpha M_{t-1} + (1 - \alpha) m_t, \quad (5)$$

where  $M_t$  is the momentum uncertainty at timestamp  $t$ , with initial value  $M_0 = 0$ . And  $\alpha \in (0, 1)$  is a hyper-parameter controlling the momentum changing.

With a recursive definition, momentum uncertainty aggregates all generated step-level uncertainties to represent the overall estimation of the reasoning process. Further, we introduce the excellent property of *momentum uncertainty* with in-depth theoretical analysis.

**Proposition 1:** *Momentum uncertainty is an exponentially weighted sum of step-level uncertainties, emphasizing recent steps and fading earlier ones.*

*Proof.* We provide a detailed derivation in Appendix A.1. It transforms Eq. (5) into the exponential weighting of step-level uncertainties as follows:

$$M_t = (1 - \alpha) \sum_{i=1}^t \alpha^{t-i} m_i. \quad (6)$$

Through Eq. (6),  $M_t$  assigns different weights  $\alpha^{t-i}$  to historical step-level uncertainty  $m_i$ , emphasizing recent uncertainties while smoothing early fluctuations, balancing the attention among different steps.

□

**Proposition 2:** *Momentum uncertainty brings more stable estimation, with lower variance than step-level uncertainty. Let  $\text{Var}(\cdot)$  denotes the variance calculation,  $\text{Var}(M_t) < \text{Var}(m_t)$ .*

*Proof.* LLM decoding contains unavoidable noise Wang et al. (2024a); Zhou et al. (2024), introducing variance to uncertainty estimation. We assume that each step-level uncertainty  $m_t$  contains two parts:

$$m_k = \mu_k + \epsilon_k, \quad \epsilon_k \sim \mathcal{N}(0, \sigma_t^2), \quad (7)$$

where  $\mu_t$  is the pure step-level uncertainty without noise, and  $\epsilon_t$  is a noise originating from training, randomly sampling, etc. And  $\mathcal{N}$  is the gaussian distribution and  $\sigma_t$  is the corresponding standard deviation.

From Eq. (7), we can infer that the variance of step-level uncertainty  $\text{Var}(m_t)$  is  $\sigma_t^2$ . Based on this assumption, we infer the variance of momentum uncertainty as follows, detailed proof is in Appendix A.2:

$$\text{Var}(M_t) = \underbrace{\frac{(1 - \alpha)(1 - \alpha^{2t})}{1 + \alpha}}_{\text{coefficient}} \sigma_t^2 < \sigma_t^2 = \text{Var}(m_t). \quad (8)$$

In Eq. (8),  $\alpha \in (0, 1)$ , making the denominator of the coefficient larger than 1 and the numerator smaller than 1. So the coefficient is between 0 and 1, making the variance of momentum uncertainty less than the variance of step-level uncertainty, leading to a more stable uncertainty estimation.

□

**Proposition 3:** *With the steps increasing, momentum uncertainty offers better convergence. Let  $\mathbb{E}[\text{Bias}(\cdot)]$  denotes the expectation of bias, then  $\mathbb{E}[\text{Bias}(M_t)] \xrightarrow{\text{converge}} 0$ .*

*Proof.* Regardless of above-mentioned noise in **Proposition 2**, LLM may still generate step-level uncertainty bias. Combining this with Eq. (6) and Eq. (7), we can infer the upper bound of momentum uncertainty bias as follows:

$$|\mathbb{E}[\text{Bias}(M_t)]| \leq K\rho^t, \quad (9)$$

where  $K$  is a finite constant,  $\rho$  is between 0 and 1. Detailed definition and proof are in Appendix A.3. This ensures rapid convergence of  $K\rho^t \rightarrow 0$  as  $t$  increases. While step-level uncertainty introduces bias, momentum-weighted uncertainty  $M_t$  effectively dampens oscillatory behavior during inference, enhancing stability.

□

Noticeably, calculating the average of step-level uncertainty is a common method Ren et al. (2022); Manakul et al. (2023); Huang et al. (2024). The theoretical superiority of our proposed  $M_t$  compared to it is in Appendix A.4. Experimental comparison is in Sec. 4.2.

### 3.3 Scalable Thinking with $\gamma$ -control

Since momentum uncertainty captures the overall confidence in the reasoning trajectory, we propose a  $\gamma$ -control mechanism to identify whether the current step is incompatible with prior reasoning. This mechanism balances reasoning performance and computational cost.

**Scale High-uncertainty Steps** At each step, the step-level uncertainty  $m_t$  reflects the model’s confidence in the current generation  $a_t$ , while  $M_{t-1}$  aggregates uncertainty over previous steps. If  $m_t > M_{t-1}$ , the current step is more uncertain than the reasoning history, suggesting it may be erroneous. To address this, we introduce a checking mechanism that selectively scales uncertain steps.

To tolerate minor fluctuations while flagging significant deviations, we apply a  $\gamma$ -control threshold. Specifically, we define a detector  $D$  in Eq. (3) as:

$$\hat{a}_t = \begin{cases} Q(\cdot|x, \mathbf{a}_{}) & , \exp(m_t) > \exp(M_{t-1})/\gamma, \\ a_t & , \text{others} \end{cases} \quad (10)$$

where  $\gamma$  is the controllable scaling rate, ranging from (0,1) in practice. The scaling factor  $\frac{1}{\gamma}$  effectively raises the detection boundary, allowing slight uncertainty increases while catching large deviations. Smaller  $\gamma$  values result in fewer steps being scaled, enabling flexible control over the computational budget.

The inequality in Eq. (10) flags when a step diverges significantly from the previous reasoning, a corrective test-time scaling is triggered to improve output quality. A theoretical analysis of  $\gamma$ -control is provided in Appendix A.5 and empirical results of  $\gamma$ -control is presented in Sec. 5.1.

**Orthogonal to Test-Time Scaling Methods** Our momentum uncertainty-based detector  $D$  is orthogonal and complementary to current test-time scaling methods, such as *best-of-N* and thinking model. It identifies uncertain steps and selectively triggers compute-intensive optimization, maintaining or even improving performance while reducing redundancy.

## 4 Experiments

### 4.1 Experimental Setup

**Benchmarks** We evaluate our proposed method *MUR* on three widely adopted math reasoning benchmarks MATH-500 [Hendrycks et al. \(2021\)](#), AIME24, and AIME25. In addition, we include GPQA-diamond [Rein et al. \(2024\)](#) to validate the generalization to the science domain.

**Metrics** We adopt pass@1 rate as our **Acc.** metric. We also report the average token usage of backbone model as **#Token** for each solution, providing an aspect of efficiency evaluation. For AIME24 and AIME25, to reduce the infection of randomness, we sample 4 times for each query and report the average accuracy.

**Test-Time Scaling Settings** We adopt three test-time scaling methods as the basic setting.

- *Guided Search*. It can be viewed as step-level *Best-of-N* [Brown et al. \(2024\)](#), where  $N$  candidate steps are sampled in parallel at each timestep, and the optimal one is selected. We adopt GenPRM 1.5B [Zhao et al. \(2025\)](#) as an external reward model for candidate selection.
- *LLM As a Critic*. The LLM receives feedback after generating each step and iteratively refines its output based on the critique [Lan et al. \(2024\)](#); [Li et al. \(2025\)](#). We also adopt GenPRM 1.5B for stepwise feedback generation.
- *$\phi$ -Decoding*. It does not require external models but selects the best step from several candidates using the foresight sampling strategy.
- *Thinking Mode*. It generates long thoughts for each step.

	MATH-500		AIME24		AIME25		GPQA-diamond		Avg.			
	Acc.↑	#Tokens ↓	Acc.↑	#Tokens ↓	Acc.↑	#Tokens ↓	Acc.↑	#Tokens ↓	Acc.↑	Δ ↑	#Tokens ↓	Δ ↓
Qwen3-1.7B												
Vanilla CoT	69.20	1,047	15.00	3,868	7.50	3,952	26.26	1,086	29.49	-	2,488	-
<b>Guided search</b>												
+ Per-Step Scale	70.80	3,460	20.83	22,498	11.67	17,882	27.27	6,739	32.64	-	12,645	-
+ Avg uncertainty	70.20	2,398	18.33	8,243	10.83	8,662	25.76	3,404	31.28	(-1.36)	5,677	(-55.10%)
+ SMART	70.80	3,128	20.83	11,887	11.67	15,845	24.74	3,825	31.96	(-0.68)	8,671	(-31.43%)
+ MUR (ours)	<b>71.20</b>	<b>1,321</b>	<b>24.17</b>	<b>6,460</b>	<b>15.83</b>	<b>5,919</b>	<b>32.83</b>	<b>2,005</b>	<b>36.01</b>	(+3.37)	<b>3,926</b>	(-68.95%)
<b>LLM as a critic</b>												
+ Per-Step Scale	70.20	1,098	19.17	4,108	9.17	3,609	28.28	<b>892</b>	31.71	-	2,427	-
+ Avg uncertainty	68.60	1,019	19.17	5,561	10.00	4,433	26.77	1,417	31.14	(-0.57)	3,108	(+28.06%)
+ SMART	70.40	878	16.67	<b>2,945</b>	10.00	<b>3,014</b>	28.28	1,446	31.34	(-0.37)	2,071	(-14.67%)
+ MUR (ours)	<b>71.20</b>	902	<b>22.50</b>	6,259	<b>10.83</b>	5,319	<b>32.32</b>	1,693	<b>34.21</b>	(+2.50)	3,543	(+45.98%)
<b>ϕ-Decoding</b>												
+ Per-Step Scale	68.00	5,501	17.50	20,518	9.17	20,629	25.76	9,261	30.11	-	13,977	-
+ Avg uncertainty	69.00	2,844	<b>19.17</b>	9,449	9.17	10,389	25.25	3,431	30.65	(+0.54)	6,278	(-55.08%)
+ SMART	<b>70.20</b>	3,848	16.67	10,992	10.00	13,693	23.23	3,338	30.02	(-0.09)	7,968	(-42.92%)
+ MUR (ours)	69.80	<b>2,520</b>	<b>19.17</b>	<b>9,180</b>	<b>12.50</b>	<b>10,016</b>	<b>27.27</b>	<b>1,827</b>	<b>32.19</b>	(+2.08)	<b>5,886</b>	(-57.89%)
Qwen3-4B												
Vanilla CoT	79.40	772	25.83	2,422	15.00	2,087	39.90	612	40.03	-	1,473	-
<b>Guided search</b>												
+ Per-Step Scale	79.80	3,048	25.83	13,445	<b>22.50</b>	12,324	42.42	3,517	42.64	-	8,084	-
+ Avg uncertainty	79.80	1,911	25.83	6,962	21.67	8,688	39.90	1,354	41.80	(-0.84)	4,729	(-41.50%)
+ SMART	<b>81.60</b>	2,476	26.67	11,087	15.83	11,604	<b>43.43</b>	2,116	41.88	(-0.76)	6,821	(-15.62%)
+ MUR (ours)	81.40	<b>824</b>	<b>28.33</b>	<b>2,791</b>	<b>22.50</b>	<b>4,009</b>	41.92	<b>929</b>	<b>43.54</b>	(+0.90)	<b>2,138</b>	(-73.55%)
<b>LLM as a critic</b>												
+ Per-Step Scale	80.80	777	30.00	4,477	17.50	2,983	40.91	737	42.30	-	2,244	-
+ Avg uncertainty	81.40	<b>741</b>	29.17	<b>2,933</b>	<b>18.33</b>	3,005	39.90	804	42.20	(-0.10)	<b>1,871</b>	(-16.58%)
+ SMART	80.60	813	26.67	3,611	16.67	2,934	<b>43.43</b>	724	41.84	(-0.46)	2,021	(-9.94%)
+ MUR (ours)	<b>81.60</b>	745	<b>30.83</b>	<b>4,561</b>	<b>18.33</b>	<b>2,531</b>	40.91	<b>699</b>	<b>42.92</b>	(+0.62)	2,134	(-4.86%)
<b>ϕ-Decoding</b>												
+ Per-Step Scale	76.80	4,690	28.33	13,483	17.50	14,378	41.41	4,263	41.01	-	9,204	-
+ Avg uncertainty	<b>80.60</b>	1,866	25.83	9,090	18.33	<b>9,752</b>	39.90	1,511	41.17	(+0.16)	5,555	(-39.65%)
+ SMART	79.40	2,776	26.67	11,671	<b>20.00</b>	12,512	40.40	2,195	41.62	(+0.59)	7,289	(-20.81%)
+ MUR (ours)	79.60	<b>1,796</b>	<b>30.00</b>	<b>4,144</b>	18.33	9,954	<b>41.92</b>	<b>944</b>	<b>42.46</b>	(+1.45)	<b>4,210</b>	(-54.26%)
Qwen3-8B												
Vanilla CoT	81.40	1,131	31.50	3,761	19.17	3,097	39.90	859	42.99	-	2,212	-
<b>Guided search</b>												
+ Per-Step Scale	<b>83.20</b>	4,069	37.50	27,672	20.83	27,871	46.46	4,252	47.00	-	15,966	-
+ Avg uncertainty	82.80	<b>2,427</b>	36.67	11,088	<b>25.00</b>	10,765	43.94	<b>2,213</b>	47.10	(+0.10)	6,623	(-58.52%)
+ SMART	82.60	3,502	37.50	15,333	21.67	17,988	<b>46.97</b>	3,797	47.19	(+0.19)	10,155	(-36.40%)
+ MUR (ours)	<b>83.20</b>	2,607	<b>40.83</b>	<b>7,930</b>	<b>25.00</b>	<b>7,972</b>	<b>46.97</b>	3,122	<b>49.00</b>	(+2.00)	<b>5,408</b>	(-66.13%)
<b>LLM as a critic</b>												
+ Per-Step Scale	83.40	<b>1,022</b>	31.67	4,472	20.83	3,886	44.44	1,172	45.09	-	2,638	-
+ Avg uncertainty	82.40	1,086	30.83	5,029	20.00	4,705	41.92	1,375	43.79	(-1.30)	3,049	(+15.58%)
+ SMART	83.20	1,167	<b>35.83</b>	<b>4,245</b>	20.00	4,125	<b>44.95</b>	1,069	46.00	(+0.91)	2,652	(+0.53%)
+ MUR (ours)	<b>83.80</b>	1,132	34.17	4,531	<b>23.33</b>	<b>3,678</b>	<b>44.95</b>	<b>1,007</b>	<b>46.56</b>	(+1.47)	<b>2,587</b>	(-1.93%)
<b>ϕ-Decoding</b>												
+ Per-Step Scale	84.20	5,841	33.33	25,181	22.50	24,555	43.43	4,726	45.87	-	15,051	-
+ Avg uncertainty	81.80	<b>3,222</b>	35.00	<b>14,233</b>	23.33	14,202	45.45	<b>2,087</b>	46.40	(+0.53)	<b>8,433</b>	(-43.97%)
+ SMART	83.20	4,782	<b>37.50</b>	20,947	20.83	21,598	44.44	4,167	46.49	(+0.62)	12,834	(-14.73%)
+ MUR (ours)	<b>84.40</b>	<b>2,854</b>	36.67	14,865	<b>25.00</b>	<b>13,719</b>	<b>47.47</b>	2,359	<b>48.39</b>	(+2.52)	8,449	(-43.86%)

Table 1: Main results. The best results are highlighted in bold. **Acc.** denotes pass@1 rate and **#Tokens** denotes the **backbone model**’s average token usage for each query, more details concerning external model token usage is in Appendix C.1. We also report the delta compared to *Per-Step Scale* method, including the accuracy difference and the percentage of saved tokens. Red indicates worse performance, while green indicates better performance. Here, ↑ denotes that lower values are better, whereas ↓ means higher values are preferable.

## Baselines

- *CoT*. Standard stepwise reasoning without scaling.
- *Per-Step Scale*. Test-time scaling methods that scale the computation for each step.
- *Avg uncertainty*. Average the uncertainty across all generated steps [Ren et al. \(2022\)](#); [Manakul et al. \(2023\)](#); [Huang et al. \(2024\)](#) to represent the overall uncertainty of the reasoning process, then scale steps with uncertainty higher than this average.
- *SMART*. Following the original work by [Kim et al. \(2025\)](#), the backbone model generates reasoning steps autonomously. If the token-level confidence (TLC) falls below a predefined threshold, we apply TTS methods.

	MATH-500		AIME24		AIME25		GPQA-diamond		Avg.			
	Acc. $\uparrow$	#Tokens $\downarrow$	Acc. $\uparrow$	$\Delta \uparrow$	#Tokens $\downarrow$	$\Delta \downarrow$						
Qwen3-1.7B												
Vanilla CoT	69.20	1,047	15.00	3,868	7.50	3,952	26.26	1,086	29.49	-	2,488	-
<b>Thinking Mode</b>												
+ Per-Step Scale	87.60	5,841	41.83	<b>14,832</b>	33.33	16,215	38.89	6,032	50.42	-	10,730	-
+ Avg uncertainty	88.80	<b>4,528</b>	42.50	14,940	30.83	16,157	39.39	5,819	50.38	<b>(-0.04)</b>	10,361	<b>(-3.44%)</b>
+ SMART	<b>89.60</b>	5,214	45.00	17,502	32.50	17,873	38.38	7,678	51.37	<b>(+0.95)</b>	12,067	<b>(+12.46%)</b>
+ MUR (ours)	<b>89.20</b>	5,041	<b>45.83</b>	16,362	<b>35.83</b>	<b>15,594</b>	<b>39.90</b>	<b>5,231</b>	<b>52.69</b>	<b>(+2.27)</b>	<b>10,557</b>	<b>(-1.61%)</b>
Qwen3-4B												
Non-Thinking Mode	79.40	772	25.83	2,422	15.00	2,087	39.90	612	40.03	-	1,473	-
<b>Thinking Mode</b>												
+ Per-Step Scale	89.20	<b>4,598</b>	70.83	13,103	57.50	16,588	51.01	6,547	67.14	-	10,209	-
+ Avg uncertainty	93.80	3,846	65.00	12,359	51.67	15,267	52.53	5,561	65.75	<b>(-1.39)</b>	9,258	<b>(-9.32%)</b>
+ SMART	<b>94.00</b>	4,932	70.00	15,088	<b>58.33</b>	17,884	53.53	8,024	68.97	<b>(+1.83)</b>	11,482	<b>(+12.47%)</b>
+ MUR (ours)	<b>94.00</b>	<b>3,607</b>	<b>75.00</b>	<b>12,117</b>	<b>58.33</b>	<b>15,202</b>	<b>54.04</b>	<b>4,801</b>	<b>70.34</b>	<b>(+3.20)</b>	<b>8,932</b>	<b>(-12.51%)</b>
Qwen3-8B												
Non-Thinking Mode	81.40	1,131	31.50	3,761	19.17	3,097	39.90	859	42.99	-	2,212	-
<b>Thinking Mode</b>												
+ Per-Step Scale	<b>94.60</b>	5,227	68.33	13,761	65.83	17,053	56.06	6,910	71.21	-	10,738	-
+ Avg uncertainty	90.60	<b>4,385</b>	63.33	<b>11,689</b>	53.33	<b>12,634</b>	55.05	6,579	65.58	<b>(-5.63)</b>	<b>8,822</b>	<b>(-17.85%)</b>
+ SMART	93.00	5,482	65.83	12,899	57.50	14,659	54.04	8,726	67.59	<b>(-3.62)</b>	10,442	<b>(-2.76%)</b>
+ MUR (ours)	93.80	5,328	<b>71.67</b>	14,390	<b>68.33</b>	17,103	<b>57.58</b>	<b>6,147</b>	<b>72.85</b>	<b>(+1.64)</b>	10,742	<b>(+0.06%)</b>

Table 2: Results of Thinking Switch. *Vanilla CoT* represents the non-thinking mode. *Per-Step Scale* here denotes the thinking mode of Qwen3 model.

**Implementation Details** We conduct all experiments on different models from Qwen3-series Yang et al. (2025a), including Qwen3-1.7B, Qwen3-4B, and Qwen3-8B. The hyper-parameter  $\alpha$  and  $\gamma$  are both set to 0.9 as default if no additional explanation is provided. For more implementation details, please to Appendix B.

## 4.2 Main Results

Table 1 and Table 2 report 4 widely adopted reasoning benchmarks across 3 sizes of models.

**MUR consistently outperforms strong baselines.** The main results demonstrate the superior token saving capacity of MUR in most scenarios, and consistently improves the accuracy against Per-Step Scale methods (from 0.62% to 3.37%). This benefits from reducing overthinking on simple steps, while keeping deliberate optimization for difficult steps.

MUR outperforms average uncertainty and SMART on both token usage and accuracy (2.20%, 1.88% for average, respectively). Although the two baselines generate fewer tokens than MUR in few cases, the accuracy drops even lower than Per-Step Scale. This indicates that they can't well evaluate the reasoning process, which laterally proves the superiority of MUR.

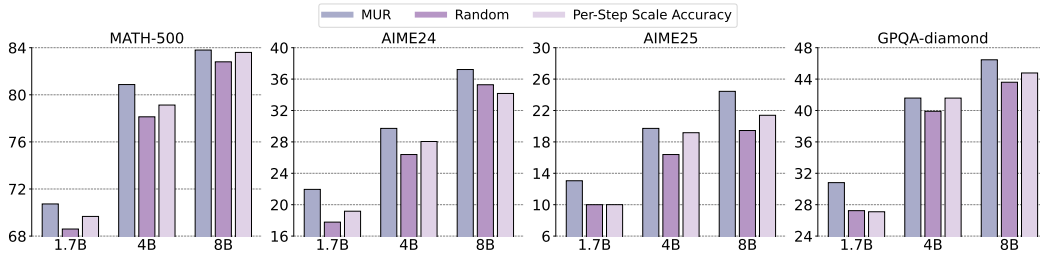


Figure 3: Random scaling accuracy. For each dataset, we average the three test-time scaling reasoning methods (Guided search, LLM as a critic,  $\phi$ -decoding). X ticks stand for different sizes of Qwen3-series models. Y stands for accuracy.

**External critic reduces backbone token usage.** For *LLM as a critic* setting, we observe that the token usage saving of the backbone is not as significant as other test-time scaling

methods. *MUR* generates 45.98% more tokens than Per-Step Scale method when using the backbone of Qwen3-1.7B, and the Per-Step Scale method even generates fewer tokens than CoT based on Qwen3-1.7B. This token usage reverse origins from the critic of external models, which contains hints for generating the next step, so the backbone generates fewer tokens. Table 1 only records the tokens generated by the backbone. To further demonstrate the token usage saving capacity of *MUR*, we report the token usage of both the backbone and the external model in Appendix C.1, from which we can observe that *MUR* is still more efficient than Per-Step Scale methods.

**Mur can generalize to LRM**s. Large reasoning models (LRMs) optimize performance by generating overlong reasoning path, leading excessive token usage. To overcome this, we directly output steps detected as needing no scaling by *MUR*, which avoids the heavy computes introduced by thinking process. More implementation details are in Appendix B.

Results in Table 2 demonstrate that *MUR* outperforms all three baselines, improving accuracy from 1.64% to 3.20% against Per-Step Scale baseline, which indicates that *MUR* adaptively identifies key steps during reasoning. Effectiveness on both reasoning models (Table 2) and non-reasoning models (Table 1) further validates the generality of *MUR*.

## 5 Analysis

In this section, we firstly present scaling law of  $\gamma$ -control (Sec. 5.1), which well balance the performance and budget. Then we analysis the number of steps and token usage (Sec. 5.2), reveling that *MUR* only scales a minor portion of steps. Finally, we randomly scale some steps (Sec. 5.3), laterally demonstrating that *MUR* can identify crucial steps. Additional analysis of the impact of hyperparameter  $\alpha$  and case study can be found in Appendix C.

### 5.1 Scaling Law of $\gamma$ -control

**$\gamma$ -control well balance performance and budget.** The hyperparameter  $\gamma$  adjusts the detection process in Eq. (10), with lower  $\gamma$  leading to less scaling and less token usage. We report this analysis in Figure 4. The accuracy improves with more token usage, indicating that we can control the reasoning performance by adjusting hyperparameter  $\gamma$ . It is worth noting that  $\gamma = \infty$  equivalents to Per-Step Scale reasoning, whose accuracy drops lower with excessive token usage. More detailed results can be found in Appendix C.2.

### 5.2 Step and Token Usage Analysis

***MUR* only scales a minor portion of steps.** We report the number of reasoning steps and corresponding token usage under different settings in Figure 5. With the guidance of *MUR*, the backbone generates 4.23-6.24 steps for average, scaling only 0.41-1.15 steps for each query. This indicates that for some simple questions, the backbone directly outputs the whole reasoning process, without any scaling.

***MUR* exhibits superior token efficiency.** *MUR* significantly reduces Per-Step Scale’s token usage over 50%. Qwen3-4B generates the least tokens, while Qwen3-8B generates the most tokens, indicating that the former is more efficient and suitable for real-world scenarios.

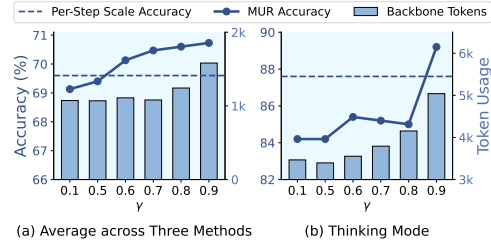


Figure 4: The scaling law of hyperparameter  $\gamma$ . We analyze MATH-500 based on Qwen-1.7B. The X axis stands for different values of  $\gamma$ . (a) reports the average of Guided search, LLM as a critic and  $\phi$ -Decoding. (b) reports the scaling law of thinking switch.

**More scaling leads to fewer token usages.** Interestingly, the number of steps is inversely proportional to total token usage—more scaling results in fewer steps, as illustrated in Figure 5. For instance, Per-Step Scale methods allocate the most tokens yet generate the fewest steps on average. This occurs because test-time scaling brings the backbone model closer to the final answer, reducing the need for future steps. Detailed statistics (Appendix C.3) reveal that harder benchmarks lead to a higher proportion of scaled steps.

### 5.3 Results of Random Scaling

**MUR identifies crucial steps to scale.** For each setting, we randomly scale the same number of steps as in Table 1 (see Appendix C.3 for details). Results in Figure 3 show the average accuracy across three Per-Step Scale methods. Random scaling underperforms Per-Step Scale by 1.02% on average, demonstrating that scaling arbitrary steps harms performance. In contrast, *MUR*—using the same number of scaled steps—outperforms both random and Per-Step Scale methods, proving its ability to identify and prioritize key reasoning steps.

## 6 Conclusion

In this paper, we emphasize the key insight that off-the-shelf test-time scaling methods allocate excessive token usage, leading to degradation of both effectiveness and efficiency. To address this, we propose *MUR*, a training-free algorithm for LLM reasoning, which can be orthogonally combined with other test-time scaling methods. We only scale key steps detected by *MUR*. Theoretical analysis and extensive experiments on both LLMs and LRM demonstrate the superiority of *MUR*. Future efforts could work on adaptively deciding how much computes to be applied on different reasoning steps.

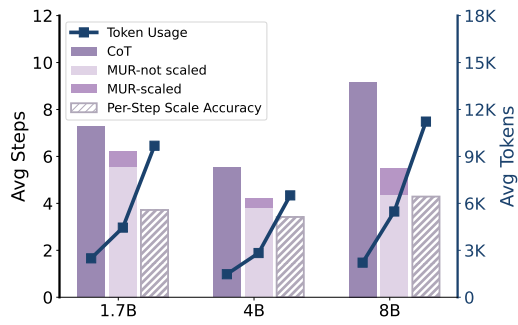


Figure 5: Comparison of average steps and token usages across different methods. Under each setting, the result is the average across all four benchmarks and the three TTS methods (Guided search, LLM as a critic,  $\phi$ -decoding). X ticks stand for different sizes of Qwen3-series models. For *MUR*, we report both the scaled steps and not scaled steps.

## References

Gustaf Ahdritz, Tian Qin, Nikhil Vyas, Boaz Barak, and Benjamin L Edelman. Distinguishing the knowable from the unknowable with language models. In *Proceedings of the 41st International Conference on Machine Learning*, pp. 503–549, 2024.

Bradley Brown, Jordan Juravsky, Ryan Ehrlich, Ronald Clark, Quoc V Le, Christopher Ré, and Azalia Mirhoseini. Large language monkeys: Scaling inference compute with repeated sampling. *arXiv preprint arXiv:2407.21787*, 2024.

Tom Brown, Benjamin Mann, Nick Ryder, Melanie Subbiah, Jared D Kaplan, Prafulla Dhariwal, Arvind Neelakantan, Pranav Shyam, Girish Sastry, Amanda Askell, et al. Language models are few-shot learners. *Advances in neural information processing systems*, 33:1877–1901, 2020.

Chao Chen, Kai Liu, Ze Chen, Yi Gu, Yue Wu, Mingyuan Tao, Zhihang Fu, and Jieping Ye. Inside: Llms’ internal states retain the power of hallucination detection. In *ICLR*, 2024a.

Jiuhai Chen and Jonas Mueller. Quantifying uncertainty in answers from any language model and enhancing their trustworthiness. In *Proceedings of the 62nd Annual Meeting of the Association for Computational Linguistics (Volume 1: Long Papers)*, pp. 5186–5200, 2024.

Xingyu Chen, Jiahao Xu, Tian Liang, Zhiwei He, Jianhui Pang, Dian Yu, Linfeng Song, Qiuzhi Liu, Mengfei Zhou, Zhuosheng Zhang, et al. Do not think that much for 2+3=? on the overthinking of o1-like llms. *CoRR*, 2024b.

Abhimanyu Dubey, Abhinav Jauhri, Abhinav Pandey, Abhishek Kadian, Ahmad Al-Dahle, Aiesha Letman, Akhil Mathur, Alan Schelten, Amy Yang, Angela Fan, et al. The llama 3 herd of models. *CoRR*, 2024.

Sebastian Farquhar, Jannik Kossen, Lorenz Kuhn, and Yarin Gal. Detecting hallucinations in large language models using semantic entropy. *Nature*, 630(8017):625–630, 2024.

Xiang Gao, Jiaxin Zhang, Lalla Mouatadid, and Kamalika Das. Spuq: Perturbation-based uncertainty quantification for large language models. In *Proceedings of the 18th Conference of the European Chapter of the Association for Computational Linguistics (Volume 1: Long Papers)*, pp. 2336–2346, 2024.

Daya Guo, Dejian Yang, Haowei Zhang, Junxiao Song, Ruoyu Zhang, Runxin Xu, Qihao Zhu, Shirong Ma, Peiyi Wang, Xiao Bi, et al. Deepseek-r1: Incentivizing reasoning capability in llms via reinforcement learning. *arXiv preprint arXiv:2501.12948*, 2025.

Dan Hendrycks, Collin Burns, Saurav Kadavath, Akul Arora, Steven Basart, Eric Tang, Dawn Song, and Jacob Steinhardt. Measuring mathematical problem solving with the math dataset. *arXiv preprint arXiv:2103.03874*, 2021.

Bairu Hou, Yujian Liu, Kaizhi Qian, Jacob Andreas, Shiyu Chang, and Yang Zhang. Decomposing uncertainty for large language models through input clarification ensembling. In *Proceedings of the 41st International Conference on Machine Learning*, pp. 19023–19042, 2024.

Xinmeng Huang, Shuo Li, Mengxin Yu, Matteo Sesia, Hamed Hassani, Insup Lee, Osbert Bastani, and Edgar Dobriban. Uncertainty in language models: Assessment through rank-calibration. In *Proceedings of the 2024 Conference on Empirical Methods in Natural Language Processing*, pp. 284–312, 2024.

Aaron Jaech, Adam Kalai, Adam Lerer, Adam Richardson, Ahmed El-Kishky, Aiden Low, Alec Helyar, Aleksander Madry, Alex Beutel, Alex Carney, et al. Openai o1 system card. *CoRR*, 2024.

Lingjie Jiang, Xun Wu, Shaohan Huang, Qingxiu Dong, Zewen Chi, Li Dong, Xingxing Zhang, Tengchao Lv, Lei Cui, and Furu Wei. Think only when you need with large hybrid-reasoning models. *arXiv preprint arXiv:2505.14631*, 2025.

Yujin Kim, Euiin Yi, Minu Kim, Se-Young Yun, and Taehyeon Kim. Guiding reasoning in small language models with llm assistance. *arXiv preprint arXiv:2504.09923*, 2025.

Lorenz Kuhn, Yarin Gal, and Sebastian Farquhar. Semantic uncertainty: Linguistic invariances for uncertainty estimation in natural language generation. In *The Eleventh International Conference on Learning Representations*, 2023.

Woosuk Kwon, Zhuohan Li, Siyuan Zhuang, Ying Sheng, Lianmin Zheng, Cody Hao Yu, Joseph E. Gonzalez, Hao Zhang, and Ion Stoica. Efficient memory management for large language model serving with pagedattention. In *Proceedings of the ACM SIGOPS 29th Symposium on Operating Systems Principles*, 2023.

Tian Lan, Wenwei Zhang, Chen Xu, Heyan Huang, Dahua Lin, Kai Chen, and Xian-Ling Mao. Criticeval: Evaluating large-scale language model as critic. *Advances in Neural Information Processing Systems*, 37:66907–66960, 2024.

Yansi Li, Jiahao Xu, Tian Liang, Xingyu Chen, Zhiwei He, Qiuwei Liu, Rui Wang, Zhuosheng Zhang, Zhaopeng Tu, Haitao Mi, et al. Dancing with critiques: Enhancing llm reasoning with stepwise natural language self-critique. *CoRR*, 2025.

Hunter Lightman, Vineet Kosaraju, Yuri Burda, Harrison Edwards, Bowen Baker, Teddy Lee, Jan Leike, John Schulman, Ilya Sutskever, and Karl Cobbe. Let’s verify step by step. In *The Twelfth International Conference on Learning Representations*, 2023.

Chang Ma, Haiteng Zhao, Junlei Zhang, Junxian He, and Lingpeng Kong. Non-myopic generation of language models for reasoning and planning. In *The Thirteenth International Conference on Learning Representations*, 2024.

Xueguang Ma, Qian Liu, Dongfu Jiang, Ge Zhang, Zejun Ma, and Wenhui Chen. General reasoner: Advancing llm reasoning across all domains. *arXiv:2505.14652*, 2025. URL <https://arxiv.org/abs/2505.14652>.

Potsawee Manakul, Adian Liusie, and Mark Gales. Selfcheckgpt: Zero-resource black-box hallucination detection for generative large language models. In *Proceedings of the 2023 Conference on Empirical Methods in Natural Language Processing*, pp. 9004–9017, 2023.

Alexander Nikitin, Jannik Kossen, Yarin Gal, and Pekka Marttinen. Kernel language entropy: Fine-grained uncertainty quantification for llms from semantic similarities. *Advances in Neural Information Processing Systems*, 37:8901–8929, 2024.

Ning Qian. On the momentum term in gradient descent learning algorithms. *Neural networks*, 12(1):145–151, 1999.

David Rein, Betty Li Hou, Asa Cooper Stickland, Jackson Petty, Richard Yuanzhe Pang, Julien Dirani, Julian Michael, and Samuel R. Bowman. GPQA: A graduate-level google-proof q&a benchmark. In *First Conference on Language Modeling*, 2024. URL <https://openreview.net/forum?id=Ti67584b98>.

Jie Ren, Jiaming Luo, Yao Zhao, Kundan Krishna, Mohammad Saleh, Balaji Lakshminarayanan, and Peter J Liu. Out-of-distribution detection and selective generation for conditional language models. In *The Eleventh International Conference on Learning Representations*, 2022.

Gaurang Sriramanan, Siddhant Bharti, Vinu Sankar Sadasivan, Shoumik Saha, Priyatham Kattakinda, and Soheil Feizi. Llm-check: Investigating detection of hallucinations in large language models. *Advances in Neural Information Processing Systems*, 37:34188–34216, 2024.

Yang Sui, Yu-Neng Chuang, Guanchu Wang, Jiamu Zhang, Tianyi Zhang, Jiayi Yuan, Hongyi Liu, Andrew Wen, Shaochen Zhong, Hanjie Chen, et al. Stop overthinking: A survey on efficient reasoning for large language models. *arXiv preprint arXiv:2503.16419*, 2025.

Sree Harsha Tanneru, Chirag Agarwal, and Himabindu Lakkaraju. Quantifying uncertainty in natural language explanations of large language models. In *International Conference on Artificial Intelligence and Statistics*, pp. 1072–1080. PMLR, 2024.

Katherine Tian, Eric Mitchell, Allan Zhou, Archit Sharma, Rafael Rafailov, Huaxiu Yao, Chelsea Finn, and Christopher D Manning. Just ask for calibration: Strategies for eliciting calibrated confidence scores from language models fine-tuned with human feedback. In *Proceedings of the 2023 Conference on Empirical Methods in Natural Language Processing*, pp. 5433–5442, 2023.

Bin Wang, Chengwei Wei, Zhengyuan Liu, Geyu Lin, and Nancy Chen. Resilience of large language models for noisy instructions. In *Findings of the Association for Computational Linguistics: EMNLP 2024*, pp. 11939–11950, 2024a.

Peiyi Wang, Lei Li, Zhihong Shao, Runxin Xu, Damai Dai, Yifei Li, Deli Chen, Yu Wu, and Zhipang Sui. Math-shepherd: Verify and reinforce llms step-by-step without human annotations. In *Proceedings of the 62nd Annual Meeting of the Association for Computational Linguistics (Volume 1: Long Papers)*, pp. 9426–9439, 2024b.

Yiming Wang, Pei Zhang, Siyuan Huang, Baosong Yang, Zhuosheng Zhang, Fei Huang, and Rui Wang. Sampling-efficient test-time scaling: Self-estimating the best-of-n sampling in early decoding. *arXiv preprint arXiv:2503.01422*, 2025.

Yangzhen Wu, Zhiqing Sun, Shanda Li, Sean Welleck, and Yiming Yang. Scaling inference computation: Compute-optimal inference for problem-solving with language models. In *The 4th Workshop on Mathematical Reasoning and AI at NeurIPS*, volume 24, 2024.

Heming Xia, Yongqi Li, Chak Tou Leong, Wenjie Wang, and Wenjie Li. Tokenskip: Controllable chain-of-thought compression in llms. *arXiv preprint arXiv:2502.12067*, 2025a.

Zhiqiu Xia, Jinxuan Xu, Yuqian Zhang, and Hang Liu. A survey of uncertainty estimation methods on large language models. *arXiv preprint arXiv:2503.00172*, 2025b.

Fangzhi Xu, Hang Yan, Chang Ma, Haiteng Zhao, Jun Liu, Qika Lin, and Zhiyong Wu.  $\phi$ -decoding: Adaptive foresight sampling for balanced inference-time exploration and exploitation. *arXiv preprint arXiv:2503.13288*, 2025a.

Fangzhi Xu, Hang Yan, Chang Ma, Haiteng Zhao, Qiushi Sun, Kanzhi Cheng, Junxian He, Jun Liu, and Zhiyong Wu. Genius: A generalizable and purely unsupervised self-training framework for advanced reasoning. *arXiv preprint arXiv:2504.08672*, 2025b.

An Yang, Anfeng Li, Baosong Yang, Beichen Zhang, Binyuan Hui, Bo Zheng, Bowen Yu, Chang Gao, Chengan Huang, Chenxu Lv, et al. Qwen3 technical report. *arXiv preprint arXiv:2505.09388*, 2025a.

Junjie Yang, Ke Lin, and Xing Yu. Think when you need: Self-adaptive chain-of-thought learning. *arXiv preprint arXiv:2504.03234*, 2025b.

Wenkai Yang, Shuming Ma, Yankai Lin, and Furu Wei. Towards thinking-optimal scaling of test-time compute for llm reasoning. *CoRR*, 2025c.

Shunyu Yao, Dian Yu, Jeffrey Zhao, Izhak Shafran, Tom Griffiths, Yuan Cao, and Karthik Narasimhan. Tree of thoughts: Deliberate problem solving with large language models. *Advances in neural information processing systems*, 36:11809–11822, 2023.

Yixin Ye, Zhen Huang, Yang Xiao, Ethan Chern, Shijie Xia, and Pengfei Liu. Limo: Less is more for reasoning. *arXiv preprint arXiv:2502.03387*, 2025.

Zhaojian Yu, Yinghao Wu, Yilun Zhao, Arman Cohan, and Xiao-Ping Zhang. Z1: Efficient test-time scaling with code. *CoRR*, 2025.

Jian Zhao, Runze Liu, Kaiyan Zhang, Zhimu Zhou, Junqi Gao, Dong Li, Jiafei Lyu, Zhouyi Qian, Biqing Qi, Li Xiu, et al. Genprm: Scaling test-time compute of process reward models via generative reasoning. *CoRR*, 2025.

Zhanke Zhou, Rong Tao, Jianing Zhu, Yiwen Luo, Zengmao Wang, and Bo Han. Can language models perform robust reasoning in chain-of-thought prompting with noisy rationales? *Advances in Neural Information Processing Systems*, 37:123846–123910, 2024.

## A Theoretical Derivation

### A.1 The Formulation of Momentum Uncertainty

**Proposition 1:** *Momentum uncertainty is an exponentially weighted sum of step-level uncertainties, emphasizing recent steps and fading earlier ones.*

*Proof.* Recursive expansion of  $M_t$ :

$$\begin{aligned}
M_t &= \alpha M_{t-1} + (1 - \alpha)m_t \\
&= \alpha(\alpha M_{t-2} + (1 - \alpha)m_{t-1}) + (1 - \alpha)m_t \\
&= \alpha^2 M_{t-2} + \alpha(1 - \alpha)m_{t-1} + (1 - \alpha)m_t \\
&\vdots \\
&= \alpha^t M_0 + (1 - \alpha) \sum_{i=1}^t \alpha^{t-i} m_i.
\end{aligned} \tag{11}$$

Substituting  $M_0 = 0$ , we obtain:

$$M_t = (1 - \alpha) \sum_{i=1}^t \alpha^{t-i} m_i. \tag{12}$$

This shows  $M_t$  assigns weights  $\alpha^{t-i}$  to historical  $m_i$ , emphasizing recent uncertainties while smoothing early fluctuations.

Let the average probability of the model's output at step  $t$ ,  $m_t$  follow  $m_t = m_{t-1} - \eta g_t$ , where  $g_t$  denotes the custom update term at step  $t$ . The momentum mechanism implicitly applies decayed weights  $1 - \alpha^{t-i}$  to historical updates.

Define cumulative updates  $m_t = m - \sum_{i=1}^{t-1} g_i$ . Substituting into Eq. (5):

$$\begin{aligned}
M_t &= \alpha M_{t-1} + (1 - \alpha)m_t \\
&= \alpha^t m_1 + (1 - \alpha) \sum_{i=1}^t \alpha^{t-i} m_i \quad (\text{from Eq. (11)}) \\
&= m_1 - \sum_{i=1}^{t-1} (1 - \alpha^{t-i}) g_i.
\end{aligned} \tag{13}$$

Compared to the baseline update  $m_t = m_1 - \sum_{i=1}^{t-1} g_i$ , the momentum term introduces weights  $1 - \alpha^{t-i}$  that decay exponentially with step distance  $t - i$ .  $\square$

From the above proof, we have two properties as following:

**Property 1:** *Momentum Uncertainty is the Exponential Weighting of Historical Uncertainties.*

**Property 2:** *Momentum Uncertainty has Gradient Descent Equivalence with Decaying Weights.*

### A.2 Proof of Low Variance

**Proposition 2:** *Momentum uncertainty brings more stable estimation, with lower variance than step-level uncertainty. Let  $\text{Var}(\cdot)$  denotes the variance calculation,  $\text{Var}(M_t) < \text{Var}(m_t)$ .*

The momentum uncertainty  $M_t$  is defined by Eq. (12) as:

$$M_t = (1 - \alpha) \sum_{i=1}^t \alpha^{t-i} m_i, \quad \alpha \in (0, 1).$$

Assume historical uncertainties  $m_t$  contain independent noise:

$$m_t = \mu_t + \epsilon_t, \quad \epsilon_t \sim \mathcal{N}(0, \sigma_t^2). \quad (14)$$

$\mu$  is the ideal value without variance and bias that can represent the current reasoning and overall reasoning path status. However, it is impractical to get  $\mu$ , and we can only get step-level uncertainty  $m$  which contains noise. Therefore, in our method, we aggregate each step-level uncertainty  $m$  as momentum uncertainty  $M$  to represent the overall reasoning process.

$$\begin{aligned} \text{Var}(M_t) &= (1 - \alpha)^2 \sum_{i=1}^t \alpha^{2(t-i)} \sigma_t^2 \\ &= (1 - \alpha)^2 \sigma_t^2 \sum_{i=1}^t \alpha^{2(t-i)}. \end{aligned} \quad (15)$$

Let  $j = t - i$ . The summation becomes a finite geometric series:

$$\begin{aligned} \sum_{i=1}^t \alpha^{2(t-i)} &= \sum_{j=0}^{t-1} \alpha^{2j} \\ &= \frac{1 - \alpha^{2t}}{1 - \alpha^2}. \end{aligned} \quad (16)$$

Substituting Eq. (16) into Eq. (15):

$$\text{Var}(M_t) = (1 - \alpha) \frac{1 - \alpha^{2t}}{1 + \alpha} \sigma_t^2. \quad (17)$$

Because  $1 - \alpha^{2t} < 1$  and  $1 + \alpha > 1$ , we have:

$$\frac{1 - \alpha^{2t}}{1 + \alpha} < 1.$$

Therefore:

$$\text{Var}(M_t) < (1 - \alpha) \cdot \sigma_t^2 \cdot 1 \leq \sigma_t^2,$$

the variance has an upper bound of  $\sigma_t^2$ .

Fix  $t$ , let  $\alpha \rightarrow 1^-$ :

$$\lim_{\alpha \rightarrow 1^-} \text{Var}(M_t) = \lim_{\alpha \rightarrow 1^-} (1 - \alpha) \sigma_t^2 \frac{1 - \alpha^{2t}}{1 + \alpha} = 0 \cdot \sigma_t^2 \cdot \frac{0}{2} = 0.$$

This shows that when  $\alpha$  is sufficiently close to 1, the variance can be arbitrarily small.

From the expression:

$$\text{Var}(M_t) = \sigma_t^2 \cdot \underbrace{(1 - \alpha) \frac{1 - \alpha^{2t}}{1 + \alpha}}_{\text{denoted as } f(\alpha, t)},$$

When  $\alpha \rightarrow 0^+$ :

$$f(\alpha, t) \rightarrow (1 - 0) \frac{1 - 0}{1 + 0} = 1.$$

When  $\alpha \rightarrow 1^-$ :

$$f(\alpha, t) \rightarrow 0.$$

For example, when we set  $\alpha = 0.9, t = 20$ :

$$f(0.9, 20) = (1 - 0.9) \frac{1 - (0.9)^{40}}{1 + 0.9} \approx 0.1 \times \frac{0.985}{1.9} \approx 0.0518.$$

The minimum occurs when  $\alpha$  approaches 1, but remains strictly greater than 0.

### A.3 Proof of Convergence

**Proposition 3:** *With the steps increasing, momentum uncertainty offers better convergence. Let  $\text{Bias}(\cdot)$  denotes the bias calculation function, then  $\text{Bias}(M_t) \xrightarrow{\text{converge}} 0$ .*

According to Eq. (14), we have  $m_t \sim \mathcal{N}(\mu_t, \sigma_t^2)$ . Therefore,

$$M_t \sim \mathcal{N}\left((1-\alpha) \sum_{i=1}^t \alpha^{t-i} \mu_i, (1-\alpha)^2 \sum_{i=1}^t \alpha^{2(t-i)} \sigma_i^2\right).$$

As claimed in Sec. A.2,  $\mu$  is the ideal value which can best represent the overall reasoning process without variance and bias, so we define the bias of  $M_t$  as:

$$\text{Bias}(M_t) = M_t - \mu_t. \quad (18)$$

Then we have:

$$\begin{aligned} \mathbb{E}[\text{Bias}(M_t)] &= \mathbb{E}[M_t - \mu_t] \\ &= \mathbb{E}[M_t] - \mu_t \\ &= (1-\alpha) \sum_{i=1}^t \alpha^{t-i} \mu_i - \mu_t. \end{aligned} \quad (19)$$

Consider non-stationary signals with drift:  $\mu_t = \mu_{t-1} + \delta_t$ . The term  $\delta_t$  represents the drift term at time  $t$ , which quantifies the change in  $\mu_t$  relative to the previous time point  $\mu_{t-1}$ . During inference, each step is generated based on previous steps, which is well compatible with this assumption.

Since  $\alpha \in (0, 1)$ , we have  $\alpha^t \in (0, 1)$ ,  $1 - \alpha^t \in (0, 1)$ .

$$\begin{aligned} (1-\alpha) \cdot \sum_{i=1}^t \alpha^{t-i} &= (1-\alpha) \cdot \frac{1 - \alpha^t}{1 - \alpha} \\ &= 1 - \alpha^t. \end{aligned} \quad (20)$$

Then we have:

$$(1-\alpha) \sum_{i=1}^t \alpha^{t-i} < 1,$$

and since  $\mu_t > 0$ , it follows that:

$$\begin{aligned} -\mu_t &< -(1-\alpha) \sum_{i=1}^t \alpha^{t-i} \mu_t. \\ \mathbb{E}[\text{Bias}(M_t)] &= (1-\alpha) \sum_{i=1}^t \alpha^{t-i} \mu_i - \mu_t \\ &< (1-\alpha) \cdot \sum_{i=1}^t \alpha^{t-i} \mu_i - (1-\alpha) \cdot \sum_{i=1}^t \alpha^{t-i} \mu_t \\ &= (1-\alpha) \cdot \sum_{i=1}^t \alpha^{t-i} \cdot (\mu_i - \mu_t). \end{aligned} \quad (21)$$

Substitute  $j = t - i$ :

$$\mathbb{E}[\text{Bias}(M_t)] < (1-\alpha) \cdot \sum_{j=0}^{t-1} \alpha^j \cdot (\mu_{t-j} - \mu_t). \quad (22)$$

As time  $t$  increases, in this asymptotic regime, the model is posited to have exhaustively explored the entirety of its accessible state space and potential cognitive trajectories. Consequently, the associated epistemic uncertainty converges to a stationary value. Assume  $\mu_i$  converges exponentially to  $\mu_\infty$  as timestamp increases:

$$|\mu_i - \mu_\infty| \leq D\beta^i, \quad \forall i \geq 1,$$

for  $D > 0$  and  $\beta \in (0, 1)$ . The constant  $D > 0$  is a scale factor for the error bound, representing the magnitude of the initial deviation, which is independent of the index  $i$ . The constant  $\beta$  is the exponential convergence rate, governing the decay speed of the error  $|\mu_i - \mu_\infty|$ . Apply the triangle inequality:

$$\begin{aligned} |\mu_{t-j} - \mu_t| &= |\mu_{t-j} - \mu_\infty + \mu_\infty - \mu_t| \\ &\leq |\mu_{t-j} - \mu_\infty| + |\mu_t - \mu_\infty| \\ &\leq D\beta^{t-j} + D\beta^t, \end{aligned} \tag{23}$$

$$\begin{aligned} |\mathbb{E}[\text{Bias}(M_t)]| &\leq (1 - \alpha) \cdot \sum_{j=0}^{t-1} \alpha^j \cdot |\mu_{t-j} - \mu_t| \\ &\leq (1 - \alpha) \cdot \sum_{j=0}^{t-1} \alpha^j \cdot (D\beta^{t-j} + D\beta^t) \\ &= (1 - \alpha) \cdot \sum_{j=0}^{t-1} D\beta^t \cdot \left( \left( \frac{\alpha}{\beta} \right)^j + \alpha^j \right) \\ &= (1 - \alpha) D\beta^t \cdot \sum_{j=0}^{t-1} \left( \left( \frac{\alpha}{\beta} \right)^j + \alpha^j \right). \end{aligned} \tag{24}$$

The second series in Eq. (24) is bounded by:

$$\sum_{j=0}^{t-1} \alpha^j = \frac{1 - \alpha^t}{1 - \alpha} \leq \frac{1}{1 - \alpha}.$$

Define  $r = \alpha/\beta$ . For the first series in Eq. (24), consider two cases:

When  $\alpha < \beta$  ( $r < 1$ ):

$$\sum_{j=0}^{t-1} r^j = \frac{1 - r^t}{1 - r} \leq \frac{1}{1 - r} = \frac{\beta}{\beta - \alpha}.$$

When  $\alpha \geq \beta$  ( $r \geq 1$ ):

$$\sum_{j=0}^{t-1} r^j = \frac{r^t - 1}{r - 1} \leq \frac{r^t}{r - 1} = \frac{\alpha^t}{\beta^{t-1}(\alpha - \beta)}.$$

Substitute the series bounds:

When  $\alpha < \beta$ :

$$\begin{aligned} |\mathbb{E}[\text{Bias}(M_t)]| &\leq (1 - \alpha) D\beta^t \left( \frac{\beta}{\beta - \alpha} + \frac{1}{1 - \alpha} \right) \\ &= D\beta^t \left( \frac{(1 - \alpha)\beta}{\beta - \alpha} + 1 \right). \end{aligned} \tag{25}$$

When  $\alpha \geq \beta$ :

$$\begin{aligned}
|\mathbb{E}[\text{Bias}(M_t)]| &\leq (1 - \alpha)D\beta^t \left( \frac{\alpha^t}{\beta^{t-1}(\alpha - \beta)} + \frac{1}{1 - \alpha} \right) \\
&= D \left[ \frac{(1 - \alpha)\alpha^t \beta}{\alpha - \beta} + (1 - \alpha)\beta^t \cdot \frac{1}{1 - \alpha} \right] \\
&= D \left( \frac{(1 - \alpha)\beta}{\alpha - \beta} \alpha^t + \beta^t \right) \\
&\leq D \left( \frac{(1 - \alpha)\beta}{\alpha - \beta} \alpha^t + \alpha^t \right) \\
&= D\alpha^t \left( \frac{(1 - \alpha)\beta}{\alpha - \beta} + 1 \right).
\end{aligned} \tag{26}$$

In both cases, we have the derived bound:

$$|\mathbb{E}[\text{Bias}(M_t)]| \leq K\rho^t, \tag{27}$$

where  $\rho = \max(\alpha, \beta)$  and  $K$  is a constant:

$$K = D \cdot \left( \frac{(1 - \alpha)\beta}{|\alpha - \beta|} + 1 \right).$$

It demonstrates that the bias converges exponentially to zero. This convergence holds because  $\rho = \max(\alpha, \beta) < 1$ , since both  $\alpha \in (0, 1)$  and  $\beta \in (0, 1)$ . The constant  $K = D \left( \frac{(1 - \alpha)\beta}{|\alpha - \beta|} + 1 \right)$  is finite and independent of  $t$ . And the exponential decay  $\rho^t \rightarrow 0$  occurs at a geometric rate.

In practice, we set  $\alpha$  close to 1, making  $(1 - \alpha)$  close to 0, minimizing  $K$ . Combined with  $\rho^t, \rho < 1$ , this ensures rapid convergence of  $K\rho^t \rightarrow 0$  as  $t$  increases. While step-level uncertainty introduces bias, momentum-weighted uncertainty  $M_t$  effectively dampens oscillatory behavior during inference, enhancing stability.

#### A.4 Proof of Superiority over Simple Average

**Proposition 4:** *Momentum uncertainty is superior to average uncertainty on both variance and bias.*

According to Eq. (6),  $M_t$  is defined as:  $M_t = (1 - \alpha) \sum_{i=1}^t \alpha^{t-i} m_i$ , and let the simple average be:

$$\tilde{M}_t = \frac{1}{t} \sum_{i=1}^t m_i. \tag{28}$$

We establish  $M_t$ 's superiority through the following analysis.

**Comparison between Momentum Average Variance and Simple Average Variance.** Historical uncertainties  $m_t$  contain independent noise is claimed in Eq. (14). The variance of  $M_t$  is derived in Eq. (17).

The vast majority of inference steps are less than twenty (as illustrated in Table 4), so  $t$  is set to  $t \leq 20$ . For  $t \leq 20$  and  $\alpha \in (0, 1)$ ,  $\alpha^{2t} \approx 0$ . Thus:

$$\text{Var}(M_t) \approx \sigma_t^2 \frac{(1 - \alpha)^2}{1 - \alpha^2} = \sigma_t^2 \frac{1 - \alpha}{1 + \alpha}. \tag{29}$$

For  $\tilde{M}_t$ :

$$\text{Var}(\tilde{M}_t) = \frac{1}{t^2} \sum_{i=1}^t \sigma_i^2 = \frac{\sigma_t^2}{t}. \tag{30}$$

When  $\alpha \rightarrow 1$ :

$$\frac{1-\alpha}{1+\alpha} < \frac{1}{t} \quad \text{for } t \leq 20, \quad (31)$$

which implies  $\text{Var}(M_t) < \text{Var}(\tilde{M}_t)$ . Momentum achieves superior noise suppression through exponentially decaying weights.

**Comparison between Momentum Average Bias and Simple Average Bias.** For the momentum uncertainty  $M_t$  illustrated in Eq. (27):

$$|\mathbb{E}[\text{Bias}(M_t)]| \leq K\rho^t.$$

For the simple average  $\tilde{M}_t$ :

$$\text{Bias}(\tilde{M}_t) = \tilde{M}_t - \mu_t = \frac{1}{t} \sum_{i=1}^t (m_i - \mu_t) \quad (32)$$

$$\mathbb{E}[\text{Bias}(\tilde{M}_t)] = \frac{1}{t} \sum_{i=1}^t (\mu_i - \mu_t) = \frac{1}{t} \sum_{i=1}^t \sum_{j=i}^t \delta_j. \quad (33)$$

It accumulates historical drifts and scales linearly with  $t$ .

Under non-stationary environments with additive noise, the momentum-based estimator  $M_t$ , exhibits superior variance-bias tradeoff and convergence properties compared to the baseline estimator  $\tilde{M}_t$ .

## A.5 Proof of Dynamic Compute Scaling

**Proposition 5:** *Optimization should be triggered with high confidence when the step-level uncertainty exhibits a significant deviation from the momentum-based uncertainty.*

**Problem Formulation and Notation** Let  $m_t$  denote the uncertainty of the model's output at step  $t+1$ , and  $M_{t-1}$  represent the momentum uncertainty defined as an exponentially weighted sum, and  $\alpha \in (0, 1)$  be the momentum rate. The decision rule for compute scaling is formulated as:

$$\exp(m_t) > \exp(M_{t-1})/\gamma.$$

A boundary violation is flagged when this inequality holds, triggering corrective test-time scaling. We formalize the robustness guarantee below.

Based on the following two lemmas, we establish that the misjudgment probability of historical momentum uncertainty  $M_{t-1}$  exceeding the threshold  $\tau_t = m_t + \ln \gamma$  approaches zero, demonstrating: When the scaling condition  $\exp(m_t) > \exp(M_{t-1})/\gamma$  holds, the model identifies abnormal elevation in current uncertainty  $m_t$  with near-certain confidence, thereby efficiently triggering resource scaling.

We now provide a theoretical bound on the probability that a stable reasoning step is mistakenly flagged as uncertain.

**Lemma 1:** *Chernoff Bound for Single Random Variable.* By using the distribution of random variables, a more precise boundary is provided for the large deviation probability of random variables.

Let  $X$  be a real-valued random variable with moment generating function  $\phi(s) = \mathbb{E}[e^{sX}]$ . For any threshold  $\tau \in \mathbb{R}$ , the upper tail probability satisfies:

$$\mathbb{P}(X \geq \tau) \leq \inf_{s>0} e^{-s\tau} \phi(s).$$

$X$  is sub-Gaussian with parameter  $\hat{\sigma}_t$ ,  $\phi(s) \leq e^{s\nu + \frac{s^2\hat{\sigma}_t^2}{2}}$ , then:

$$\mathbb{P}(X \geq \tau) \leq \exp\left(-\frac{(\tau - \nu)^2}{2\hat{\sigma}_t^2}\right),$$

where  $\nu = \mathbb{E}[X]$ .

$$\tau_t = m_t + \ln(\gamma), \quad \gamma \in (0, 1).$$

**Lemma 2:** *Hoeffding's inequality.* Hoeffding's inequality provides the upper limit of the probability that the sum of a random variable deviates from its expected value.

Assume that for each  $i$ ,  $X_i \in [a_i, b_i]$ . Consider the sum of these random variables:

$$S_n = \sum_{i=1}^n X_i = X_1 + X_2 + X_3 + \cdots + X_{n-1} + X_n.$$

Then Hoeffding's inequality states that for all  $t > 0$ :

- $\mathbb{P}(S_n - \mathbb{E}[S_n] \geq t) \leq \exp\left(-\frac{2t^2}{\sum_{i=1}^n (b_i - a_i)^2}\right).$
- $\mathbb{P}(|S_n - \mathbb{E}[S_n]| \geq t) \leq 2 \exp\left(-\frac{2t^2}{\sum_{i=1}^n (b_i - a_i)^2}\right).$

Here  $\mathbb{E}[S_n]$  denotes the expectation of  $S_n$ .

Let the momentum uncertainty sequence  $M_{t-1}$  be an exponentially weighted sum of historical step-level uncertainties  $\{m_i\}_{i=1}^{t-1}$ :

$$M_{t-1} = \sum_{i=1}^{t-1} \omega_i m_i, \quad \omega_i = \alpha^{t-1-i} (1 - \alpha), \quad \sum_{i=1}^{t-1} \omega_i = 1,$$

where  $m_i \in [0, 1]$  are bounded random variables. The threshold has been defined above, which is:

$$\tau_t = m_t + \ln \gamma.$$

When the scaling condition  $\exp(m_t) > \exp(M_{t-1})/\gamma$  holds, applying **Lemma 1**, we have:

$$\mathbb{P}(M_{t-1} \geq \tau_t) \leq \exp\left(-\frac{(\tau_t - \hat{v}_{t-1})^2}{2\hat{\sigma}_{t-1}^2}\right),$$

where  $\hat{v}_{t-1} = \mathbb{E}[M_{t-1}]$ , and the decay rate is controlled by  $\alpha$ .

*Proof.* By the exponential smoothing definition:

$$M_{t-1} = \sum_{i=1}^{t-1} \omega_i m_i, \quad \omega_i = (1 - \alpha)\alpha^{t-1-i},$$

where  $m_i \in [0, 1]$  are independent or weakly dependent random variables. Define  $X_i = \omega_i m_i$ , which satisfies:

- $X_i \in [0, \omega_i]$ .
- $b_i - a_i = \omega_i - 0 = \omega_i$ .

Applying **Lemma 2**:

$$\begin{aligned} \mathbb{P}[\exp(M_{t-1} - \mathbb{E}[M_{t-1}]) \geq \zeta] &\leq \exp\left(-\frac{2\zeta^2}{\sum_{i=1}^{t-1} (b_i - a_i)^2}\right) \\ &= \exp\left(-\frac{2\zeta^2}{\sum_{i=1}^{t-1} \omega_i^2}\right). \end{aligned}$$

$M_{t-1}$  is sub-Gaussian with parameter:  $\hat{\sigma}_{t-1}^2 = \frac{1}{4} \sum_{i=1}^{t-1} \omega_i^2$ . Thus:

$$\mathbb{P}(M_{t-1} - \hat{v}_{t-1} \geq \zeta) \leq \exp\left(-\frac{\zeta^2}{2\hat{\sigma}_{t-1}^2}\right). \quad (34)$$

Substitute  $\zeta = \tau_t - \hat{v}_{t-1}$ :

$$\begin{aligned}
\mathbb{P}(M_{t-1} \geq \tau_t) &\leq \exp\left(-\frac{(\tau_t - \hat{v}_{t-1})^2}{2 \cdot \frac{1}{4} \sum_{i=1}^{t-1} \omega_i^2}\right) \\
&= \exp\left(-\frac{(\tau_t - \hat{v}_{t-1})^2}{2 \cdot \frac{1}{4} ((1-\alpha)^2 \sum_{j=0}^{t-2} (\alpha^2)^j)}\right) \\
&= \exp\left(-\frac{(\tau_t - \hat{v}_{t-1})^2}{2 \cdot \frac{1}{4} ((1-\alpha)^2 \cdot \frac{1-\alpha^{2(t-1)}}{1-\alpha^2})}\right) \\
&= \exp\left(-\frac{2(\tau_t - \hat{v}_{t-1})^2(1+\alpha)}{(1-\alpha)(1-\alpha^{2(t-1)})}\right) \\
&= \exp\left(-\frac{2(m_t + \ln \gamma - \hat{v}_{t-1})^2(1+\alpha)}{(1-\alpha)(1-\alpha^{2(t-1)})}\right). \tag{35}
\end{aligned}$$

Since  $1 - \alpha^2 = (1 - \alpha)(1 + \alpha)$ ,  $\alpha \in (0, 1)$ :

$$\sum_{i=1}^{t-1} \omega_i^2 = (1 - \alpha) \cdot \frac{1 - \alpha^{2(t-1)}}{1 + \alpha} \leq \frac{1 - \alpha}{1 + \alpha}.$$

Substituting the weight sum upper bound:

$$\mathbb{P}(M_{t-1} \geq \tau_t) \leq \exp\left(-\frac{2(m_t + \ln \gamma - \hat{v}_{t-1})^2(1+\alpha)}{1-\alpha}\right). \tag{36}$$

□

As those in practice, we set  $\alpha = 0.9$  in the probability bound here:

$$\begin{aligned}
\mathbb{P}(M_{t-1} \geq \tau_t) &\leq \exp\left(-\frac{2(m_t + \ln \gamma - \hat{v}_{t-1})^2(1+\alpha)}{1-\alpha}\right) \\
&= \exp\left(-38(m_t + \ln \gamma - \hat{v}_{t-1})^2\right) \rightarrow 0.
\end{aligned}$$

Define the confidence parameter  $\varepsilon$  as:

$$\varepsilon = \exp\left(-\frac{2(\ln \gamma + m_t - \hat{v}_{t-1})^2(1+\alpha)}{1-\alpha}\right).$$

This exponential decay ensures that deviations above  $\tau_t = \ln \gamma + m_t$  are asymptotically improbable. With  $\alpha = 0.9$ , the bound becomes:  $\varepsilon = \exp(-38(\ln \gamma + m_t - \hat{v}_{t-1})^2) \rightarrow 0$ ,

$$\begin{aligned}
\mathbb{P}(M_{t-1} \geq \tau_t) &= \varepsilon \rightarrow 0, \\
\mathbb{P}(M_{t-1} < \tau_t) &= \mathbb{P}\left(\exp(m_t) > \frac{\exp(M_{t-1})}{\gamma}\right) \\
&= 1 - \varepsilon.
\end{aligned}$$

This validates the scaling decision: **The scaling condition  $\exp(m_t) > \exp(M_{t-1})/\gamma$  holds with confidence  $1 - \varepsilon$ .** This result establishes generalization error control for exponential smoothing: The weighted average  $M_{t-1}$  converges to the expected uncertainty level, while the scaling condition controls abrupt deviations via tail probability analysis.

## B Implementation Details

**Implementation of Main Experiments** The temperature is set to 0.6 for all experiments. In practice, we do not scale the first step. Because there is no valid momentum uncertainty when identifying the first step. For math problem evaluation, We conduct all of our experiments based on vLLM [Kwon et al. \(2023\)](#) reasoning tool. We use general reasoner [Ma et al. \(2025\)](#) for math problem evaluation.

**Implementation of Generating One Step** For generating one step, we prompt the backbone LLM to automatically define one step. Specifically, we add *Always end your solution with the phrase “the answer is” followed by your final answer. Start your solution with “Step {stepidx}:”* to the end of each input query. For the update of momentum uncertainty, we use the step-level uncertainty of optimized step.

**Implementation of Thinking Switch** Based on the switch interface between non-thinking mode and thinking mode provided by Qwen3-series, we propose to reduce token usage for large reasoning models with *MUR*. Specifically, we use non-thinking mode as default reasoning method, and switch to thinking mode when current step is detected as needing scaling by *MUR*. We set  $\gamma$  to 0.9, 0.8, 0.7 for MATH, AIME, GPQA-diamond, respectively. To avoid overthinking in each step, we limit the max thinking length to 2048 and extract all the completed sentences. Additionally, we add “Okay, so I need to” to the beginning of each prompt to correctly elicit thinking in thinking mode.

## C More Experiment Results

### C.1 Token Usage

We report the token usage of both the backbone and the external model in Table 3. There is no external model under  $\phi$ -Decoding setting, so we only report the token usage under Guided search and LLM as a critic settings. In Table 1, *MUR* generates more tokens in some cases. This is because we only record the backbone token usage in Table 1. However, in Table 3, by adding up both backbone token usage and external model token usage, we can observe in the last column that *MUR* consistently generates fewer tokens than Per-Step Scale method, validating the token saving capacity of *MUR*. Furthermore, the trend of token usage of the Guided search setting in Table 3 is compatible with those in Table 1.

### C.2 Flexible Control with Hyperparameter $\gamma$

To further demonstrate the flexible control using hyperparameter  $\gamma$ , we report the detailed information concerning three model sizes and four test-time scaling methods (Guided search, LLM as a critic,  $\phi$ -Decoding, thinking switch) on MATH-500 in Figure 6. It can be observed that by increasing  $\gamma$ , the reasoning accuracy would improve along with the token usage.

It is worth noting that in some scenarios, we observe performance degradation when we set  $\gamma$  to 0.9. This is consistent with our main findings: the reasoning performance drops with excessive reasoning token usage. In other words, we scale abundant steps in these scenarios. And the accuracy of Per-Step Scale methods drops even lower with more token usage. Additionally, we observe that *MUR* outperforms Per-Step Scale in most scenarios. In practice, we set  $\gamma$  to 0.9 as the default.

### C.3 Number of Steps

We report the number of steps generated by the backbone model and the number of scaled steps with *MUR* in Table 4. Additionally, we calculate the percentage of scaled steps on each benchmark. For MATH-500, AIME24, AIME25, GPQA-diamond, the percentage is 8.38%, 13.19%, 17.83%, 13.75%, respectively. We can infer that among them, more difficult benchmark leads to higher percentage of scaled steps.

### C.4 Impact of $\alpha$

The hyperparameter  $\alpha$  controls the update of momentum uncertainty, with a lower  $\alpha$  leading to more intense updates. We report the impact of changing  $\alpha$  in Figure 7. We can observe that *MUR* outperforms vanilla in most cases, which demonstrates the insensitivity and effectiveness of *MUR*. For  $\alpha = 0.1$  setting, the momentum uncertainty changes too fast

	MATH-500			AIME24			AIME25			GPQA-diamond			Avg.		
	Bac↓	Ext↓	Sum↓	Bac↓	Ext↓	Sum↓	Bac↓	Ext↓	Sum↓	Bac↓	Ext↓	Sum↓	Bac↓	Ext↓	Sum↓
Qwen3-1.7B															
CoT	1,047	-	1,047	3,868	-	3,868	3,952	-	3,952	1,086	-	1,086	2,488	-	2,488
Guided search															
+ Per-Step Scale	3,460	3,186	6,646	22,498	23,055	45,553	17,882	17,859	35,741	6,739	9,258	15,997	12,645	13,339	25,984
+ Avg uncertainty	2,398	1,565	3,963	8,243	3,219	11,462	8,662	3,558	12,220	3,404	3,512	6,916	5,677	2,964	8,641
+ SMART	3,128	2,049	5,177	11,887	10,722	22,609	15,845	13,112	28,957	3,825	5753	9,578	8,671	7,909	16,580
+ MUR (ours)	1,321	320	1,641	6,460	896	7,356	5,919	1,263	7,182	2,005	1,502	3,507	3,926	995	4,921
LLM as a critic															
+ Per-Step Scale	1,098	1,271	2,369	4,108	1,877	5,985	3,609	1,737	5,346	892	2,249	3,141	2,427	1,783	4,210
+ Avg uncertainty	1,019	1,075	2,094	5,561	611	6,172	4,433	660	5,093	1,417	2,001	3,418	3,108	1,087	4,194
+ SMART	878	670	1,548	2,945	1,676	4,621	3,014	1,542	4,556	1,446	763	2,209	2,071	1,163	3,234
+ MUR (ours)	902	337	1,239	6,259	483	6,742	5,319	542	5,861	1,693	1,282	2,975	3,543	661	4,204
Qwen3-4B															
CoT	772	-	772	2,422	-	2,422	2,087	-	2,087	612	-	612	1,473	-	1,473
Guided search															
+ Per-Step Scale	3,048	3,346	6,394	13,445	13,229	26,674	12,324	15,464	27,788	3,517	6,437	9,954	8,084	9,619	17,703
+ Avg uncertainty	1,911	1,845	3,756	6,962	3,416	10,378	8,688	3,836	12,524	1,354	2,483	3,837	4,729	2,895	7,624
+ SMART	2,476	2,212	4,688	11,087	13,784	24,871	11,604	13,830	25,434	2,116	3,409	5,525	6,821	8,309	15,130
+ MUR (ours)	824	265	1,089	2,791	1,863	4,654	4,009	1,702	5,711	929	641	1,570	2,138	1,118	3,256
LLM as a critic															
+ Per-Step Scale	777	1,373	2,150	4,477	2,757	7,234	2,983	1,867	4,850	737	2,462	3,199	2,244	2,115	4,359
+ Avg uncertainty	741	957	1,698	2,933	622	3,555	3,005	900	3,905	804	1,795	2,599	1,871	1,069	2,940
+ SMART	813	855	1,668	3,611	1,089	4,700	2,934	1,094	4,028	724	320	1,044	2,021	839	2,860
+ MUR (ours)	745	443	1,188	4,561	1,893	6,454	2,531	1,447	3,978	699	266	965	2,134	1,012	3,146
Qwen3-8B															
CoT	1,131	-	1,131	3,761	-	3,761	3,097	-	3,097	859	-	859	2,212	-	2,212
Guided search															
+ Per-Step Scale	4,069	3,688	7,757	27,672	18,843	46,515	27,871	16,090	43,961	4,252	7,468	11,720	15,966	11,522	27,488
+ Avg uncertainty	2,427	2,037	4,464	11,088	4,139	15,227	10,765	4,367	15,132	2,213	3,382	5,595	6,623	3,481	10,104
+ SMART	3,502	3,287	6,789	15,333	6,221	21,554	17,988	7,094	25,082	3,797	6,135	9,932	10,155	5,684	15,839
+ MUR (ours)	2,607	1,986	4,593	7,930	1,715	9,645	7,972	2,026	9,998	3,122	4,524	7,646	5,408	2,563	7,971
LLM as a critic															
+ Per-Step Scale	1,022	2,025	3,047	4,472	2,612	7,084	3,886	2,691	6,577	1,172	3,102	4,274	2,638	2,608	5,246
+ Avg uncertainty	1,086	842	1,928	5,029	1,137	6,166	4,705	1,392	6,097	1,375	1,588	2,963	3,049	1,240	4,289
+ SMART	1,167	1,160	2,327	4,245	1,769	6,014	4,125	2,177	6,302	1,069	2,366	3,435	2,652	1,868	4,520
+ MUR (ours)	1,132	783	1,915	4,531	1,953	6,484	3,678	2,120	5,798	1,007	2,211	3,218	2,587	1,767	4,354

Table 3: Token usage of both backbone and external model. **Bac** stands for backbone model, **Ext** stands for external model, and the sum of them is denoted as **Sum**. ↓ means better for lower values.

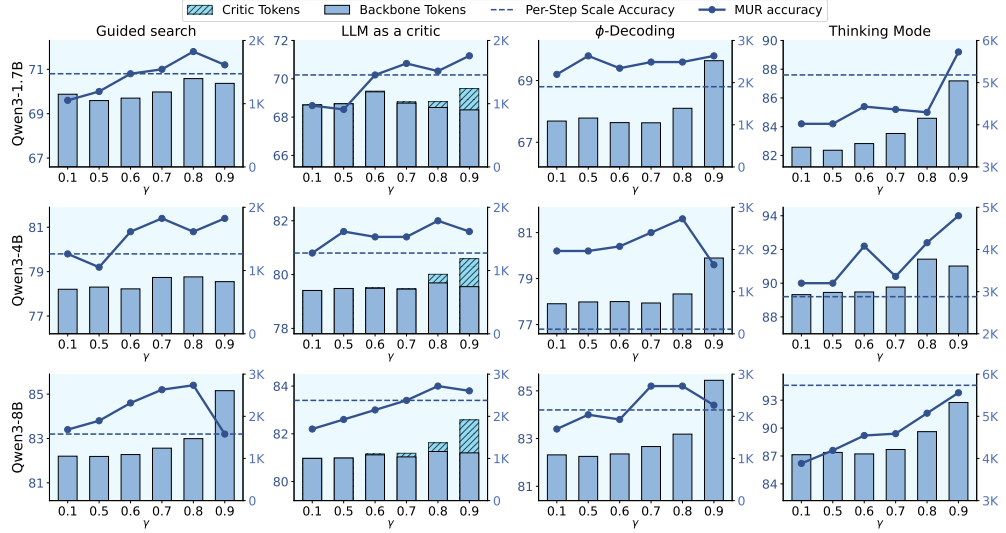


Figure 6: Detail scaling law of  $\gamma$ . The X axis stands for different values of  $\gamma$ . The Y axis stands for accuracy. Due to the reason described in Appendix C.1, we additionally report the external model token usage (denoted as Critic Tokens) under LLM as a critic setting to comprehensively reflect the overall computes.

to well represent the overall estimation of query and generated steps, so the accuracy is relatively lower than other settings. In practice, we set  $\alpha = 0.9$  as default.

Datasets	MATH-500		AIME24		AIME25		GPQA-diamond		Avg	
	Total	Scaled	Total	Scaled	Total	Scaled	Total	Scaled	Total	Scaled
Qwen3-1.7B										
CoT	5.33	-	8.93	-	8.40	-	6.41	-	7.27	-
Guided search										
+ Per-Step Scale	2.89	2.89	4.03	4.03	2.97	2.97	4.55	4.55	3.61	3.61
+ MUR (ours)	5.31	0.35	6.60	0.57	6.27	0.70	7.02	0.82	6.30	0.61
LLM as a critic										
+ Per-Step Scale	4.35	4.35	4.40	4.40	3.87	3.87	3.93	3.93	4.14	4.14
+ MUR (ours)	5.86	0.40	6.63	0.87	6.00	0.97	5.77	0.81	6.07	0.76
$\phi$ -Decoding										
+ Per-Step Scale	2.97	2.97	3.10	3.10	3.67	3.67	3.91	3.91	3.41	3.41
+ MUR (ours)	5.80	0.39	7.57	0.53	6.53	0.70	5.59	0.76	6.37	0.60
Qwen3-4B										
CoT	5.84	-	5.70	-	5.00	-	5.57	-	5.53	-
Guided search										
+ Per-Step Scale	2.73	2.73	3.20	3.20	3.80	3.80	2.71	2.71	3.11	3.11
+ MUR (ours)	4.31	0.17	4.20	0.23	4.40	0.67	3.59	0.30	4.13	0.34
LLM as a critic										
+ Per-Step Scale	3.83	3.83	3.80	3.80	4.50	4.50	2.47	2.47	3.65	3.65
+ MUR (ours)	4.36	0.18	5.00	0.33	4.07	0.57	3.31	0.35	4.19	0.36
$\phi$ -Decoding										
+ Per-Step Scale	2.77	2.77	3.43	3.43	4.63	4.63	3.10	3.10	3.48	3.48
+ MUR (ours)	4.38	0.19	5.23	0.60	4.30	0.30	3.89	1.02	4.45	0.53
Qwen3-8B										
CoT	7.45	-	10.00	-	12.33	-	6.90	-	9.17	-
Guided search										
+ Per-Step Scale	3.27	3.27	3.80	3.80	3.93	3.93	3.83	3.83	3.71	3.71
+ MUR (ours)	5.32	0.40	6.43	1.00	6.43	1.03	5.20	0.69	5.85	0.78
LLM as a critic										
+ Per-Step Scale	5.01	5.01	4.60	4.60	4.17	4.17	3.92	3.92	4.43	4.43
+ MUR (ours)	5.93	0.55	6.53	1.00	6.77	1.27	5.17	0.67	6.10	0.87
$\phi$ -Decoding										
+ Per-Step Scale	3.20	3.20	3.70	3.70	6.07	6.07	3.45	3.45	4.11	4.11
+ MUR (ours)	4.45	1.20	4.83	1.60	4.80	2.27	4.32	2.11	4.60	1.80

Table 4: Total number of steps generated by the backbone and the number of scaled steps with *MUR*.

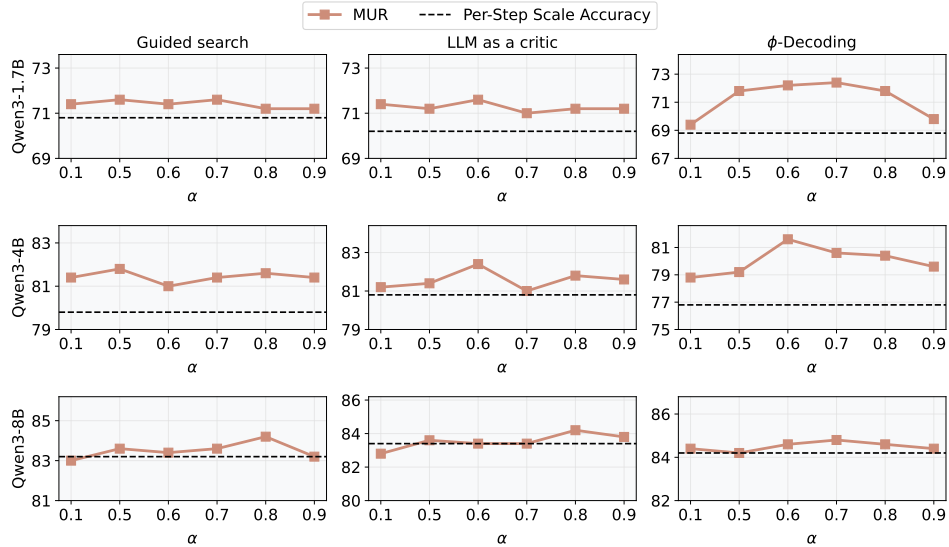


Figure 7: Impact of changing  $\alpha$ . The X axis stands for different values of  $\alpha$ . The Y axis stands for accuracy.

## C.5 Case Study

In Figure 8, we conduct a case study based on the thinking mode of Qwen3-1.7B. We analyze AIME24 and show the comparison between *MUR* and Per-Step Scale. We can observe that when *MUR* faces high uncertainty step, it triggers the thinking process, allocating more

computes to optimize current step's quality. For simple steps showing low uncertainty, *MUR* directly output it without thinking. On the contrary, *Per-Step Scale* thinks for every step, regardless of whether the backbone is confident with the current step or not.

<p>Question: Eight circles of radius 34 are sequentially tangent, and two of the circles are tangent to <math>AB</math> and <math>BC</math> of triangle <math>ABC</math>, respectively. 2024 circles of radius 1 can be arranged in the same manner. The inradius of triangle <math>ABC</math> can be expressed as <math>m/n</math>, where <math>m</math> and <math>n</math> are relatively prime positive integers. Find <math>m+n</math>.</p> <p>Ground Truth: 197</p>	
<p><b>MUR</b></p> <p>Step1: Okay, so I need to find the inradius of triangle ABC...</p> <p>Step2(Before Scale): First, I need to visualize the problem ... But they are tangent to AB and BC. <b>Hmm.</b></p> <div style="background-color: #e0e0ff; padding: 5px; border-radius: 10px; text-align: center;"> <b>NEED SCALING!!!</b>  <math>[\exp(m)=1.32, \exp(M)/\gamma=1.26]</math> </div> <p>Step2(After Scale): &lt;think&gt; <b>Alternatively</b>, maybe they are arranged in a way similar to the incircle and excircle? But with circles of radius 34 ... Therefore, maybe the circles are tangent to AB or BC, and the other side? &lt;/think&gt;</p> <p>Step3: The problem says "eight circles of radius 34 are sequentially tangent, and two of the circles are tangent to AB and BC of triangle ABC, respectively..."</p> <p>... [omit some intermediate steps] ...</p> <p>Step8(Before Scale): But I <b>don't know theta</b>, so this seems stuck.</p> <div style="background-color: #e0e0ff; padding: 5px; border-radius: 10px; text-align: center;"> <b>NEED SCALING!!!</b>  <math>[\exp(m)=1.56, \exp(M)/\gamma=1.37]</math> </div> <p>Step8(After Scale): &lt;think&gt; <b>But</b> if we have two different arrangements ... Therefore, the inradius is <math>192/5</math>, so <math>m + n = 192 + 5 = 197</math>. Therefore, the inradius is <math>192/5</math>, so <math>m + n = 192 + 5 = 197</math>. <b>Final Answer</b> <b>197</b> &lt;/think&gt;</p> <p>To determine the inradius of triangle ABC, we analyze the geometric arrangement of circles of two different radii ... Final Answer <math>m = 192, n = 5, m + n = 197</math></p>	<p><b>Per-Step Scale</b></p> <p>Step1(Before Scale): Okay, so I need to find the inradius of triangle ABC...</p> <p>Step1(After Scale): &lt;think&gt; First, let me try to visualize the problem. There's triangle ABC ... Because in the right triangle formed by B, the center, and the foot of the perpendicular from the center to AB, we have <math>\sin(\theta/2) = \text{opposite} / \text{hypotenuse} = 34 / d</math>.&lt;/think&gt;</p> <p>Step2(Before Scale): So <math>d = 34 / \sin(\theta/2)</math>.</p> <p>Step2(After Scale): &lt;think&gt; If there are two circles tangent to AB and BC, and they are tangent to each other ... if the circles are arranged in a triangle with inradius R, then maybe <math>R = r * k</math>, where k is the scaling factor. If we can find k, then we can compute R.&lt;/think&gt;</p> <p>Step3(Before Scale): <b>But how?</b></p> <p>Step3(After Scale): &lt;think&gt; <b>Alternatively</b>, think of the problem as similar to a triangle with inradius R, and circles of radius r arranged inside it ... But since the last circle is also tangent to AB and BC, its distance from B is <math>d - n = 34 / \sin(\theta/2)</math>.&lt;/think&gt;</p> <p>... [omit some intermediate steps] ...</p> <p>Step5(Before Scale): Think of the triangle as having a certain inradius R, and each circle of radius r is placed such that it touches two sides and the inradius...</p> <p>Step5(After Scale): &lt;think&gt; But this is too vague ... Therefore, this is not possible. Given that I'm stuck, and the only possible answer I can think of is <math>34/253</math>, leading to <math>m + n = 287</math>, I will go with that.</p> <p><b>Final Answer</b> <b>287</b> &lt;/think&gt;</p> <p>To solve this problem, we are given two sets of circles...Thus, <math>m + n = 34 + 253 = 287</math></p>

Figure 8: Case study. **Red** denotes the backbone faces high uncertain step. **Green** denotes key words of thinking.